



ELSEVIER

Available online at [www.sciencedirect.com](http://www.sciencedirect.com)

SCIENCE @ DIRECT®

Journal of Sound and Vibration 285 (2005) 1109–1122

JOURNAL OF  
SOUND AND  
VIBRATION

[www.elsevier.com/locate/jsvi](http://www.elsevier.com/locate/jsvi)

# Wheat stem moduli in vivo via reference basis model updating

Jiang Zhou<sup>a</sup>, Tony Farquhar<sup>b,\*</sup>

<sup>a</sup>*Department of Mechanical Engineering, Lamar University, Beaumont, TX 77710, USA*

<sup>b</sup>*Department of Mechanical Engineering, University of Maryland, 1000 Hilltop Circle, Baltimore County, MD 21250, USA*

Received 18 June 2003; received in revised form 10 September 2004; accepted 15 September 2004  
Available online 24 December 2004

## Abstract

A novel structural analysis method was developed and used to infer the in vivo material properties of an important crop species. In particular, reference basis model updating was used to reconcile the predictions of an idealized analytical model with the observed forced vibration response of living wheat, and thereby determine the effective longitudinal moduli of the tissues comprising the vibrating structure. The ensuing study of two varieties of wheat found that the stem tissue moduli decreased nonlinearly with height. These findings were in good qualitative agreement with the limited data available in the literature, and the updating procedure was highly effective in this unusual nondestructive testing application. To our knowledge, this is the first time that the reference basis method has been used to infer the spatially varying material properties of a living plant. Moreover, similar approaches could be used to characterize spatial variations in the material properties of other lightweight composite structures of arbitrary geometry.

© 2004 Elsevier Ltd. All rights reserved.

## 1. Introduction

Wheat is one of the major crops of global agriculture and provides 20% of total human caloric intake. A wheat stalk can be idealized as a slender vertical cantilever supporting a relatively massive tip load. The stalk consists of a segmented hollow stem supporting a grain-bearing flower or spike. A wheat crop is continually subjected to the forces of gravity and wind, and the economic value of grain lost due to wind-induced crop failure has been estimated to be \$8 billion per year [1]. Crop scientists are therefore very interested in the mechanical properties of wheat.

\*Corresponding author. Tel.: +1 410 4553339; fax: +1 410 4551052.  
E-mail address: [farquhar@umbc.edu](mailto:farquhar@umbc.edu) (T. Farquhar).

There is some evidence that the mechanical properties of the wheat stem vary along its vertical axis [2–5], but it is difficult to obtain a truly realistic measure of its effective elastic properties. In fact, the reported values of the longitudinal Young's moduli based on static testing of dried wheat stem specimens span more than an order of magnitude [3,4,6–8]. Other estimates of the stem elastic properties have been based on dynamic frequency response [2,9,10] or on ultrasonic wavespeed [5]. While these earlier studies provided useful information, it is difficult to assess the accuracy of the results. In contrast, the present study describes a new method that allows the stem tissue moduli to be determined more accurately as a step-wise function of height. In particular, a model updating scheme called the reference basis method is used to obtain a set of elastic moduli, which is simultaneously consistent with the predictions of an idealized analytical model and with the observed structural response.

Much effort in engineering analysis has been devoted to the development of mathematical models of a physical system. In practice, there are usually some inconsistencies between theory and experiment. For example, the theory may neglect certain dof, it may incorrectly represent boundary conditions, or it relies on imprecise knowledge of structural geometry and/or material properties. Similarly, the experimental response may be confounded by experimental artifact or by instrument inaccuracies. In most cases, one seeks a model that is most consistent with all the available information rather than an exact match to either theory or experiment. Model updating is one approach that can be used to achieve this goal. A number of specific updating techniques have been proposed and investigated. These include system identification, sensitivity methods, and mixed matrix approaches, as well as various so-called reference basis methods [11]. The reference basis concept was first popularized by Baruch [12,13] and Berman [14] in the late 1970s. Typically, experimental knowledge of one physical quantity (e.g., mass) is assumed to be perfectly accurate, while other parameters (e.g., stiffness, modes) are assumed to be known in a more approximate sense, and are therefore updated to reduce model inconsistency. Another version of this approach [15] uses general weighting functions and demonstrates the underlying parallel between reference basis and mixed matrix methods. One advantage of the reference basis approach is that a closed-form solution can be obtained using low-order matrix algebra. Another is that mass can usually be measured with great accuracy, and therefore establishes the best reference basis from which to search for the unknown stiffness. Sensitivity methods could also be used but cannot leverage the superior accuracy of the mass data.

In the present work, the motivation for use of reference basis model updating was to infer the elastic moduli of a living wheat stem. As far as we know, this is the first time that *in vivo* material property data have been obtained in this way from nondestructive frequency testing of a living plant.

## 2. Reference basis method

### 2.1. Problem statement

First, let  $M_T$  and  $K_T$  be the exact mass and stiffness matrices, respectively, for a forced system with  $n$  degrees of freedom. The *true* equation of motion is

$$[M_T]\{\ddot{x}\} + [K_T]\{x\} = \{f(t)\}. \quad (1)$$

The term *true* here is understood to mean very accurate within the framework established by the available data and the ultimate purpose of the analysis. The associated natural frequencies and mode shapes of this system are  $\omega_{Ti}$  and  $\phi_{Ti}$ , respectively, where  $i = 1$  to  $n$ . Subscript  $T$  here implies true model.

Second, let  $M_A$  and  $K_A$  be the analytical mass and stiffness matrices, respectively, perhaps obtained using a finite element model or by some other method. Thus, the analytical equation of motion of the system is

$$[M_A]\{\ddot{x}\} + [K_A]\{x\} = \{f(t)\}. \tag{2}$$

In general, the true and the corresponding analytical quantities are not exactly the same. However, in our case, we assume that  $M_A = M_T \equiv M$  to simplify the discussion, since the mass can be measured with the highest accuracy.

Third, let the resonant frequencies and mode shapes obtained from modal testing be  $\omega_{Ei}$  and  $\phi_{Ei}$ , respectively, where  $i = 1$  to  $m$  and  $m \leq n$ . Subscript  $E$  here implies experimental model. In matrix notation, the diagonal frequency matrix is

$$\Omega_E = \begin{bmatrix} \omega_{E1} & & & \\ & \omega_{E2} & & \\ & & \dots & \\ & & & \omega_{Em} \end{bmatrix} \tag{3}$$

and the  $n \times m$  mode shape matrix is

$$\Phi_E = [\Phi_{E1} \cdots \Phi_{Em}]. \tag{4}$$

In many situations, it is reasonable to assume that the measured frequencies are very close to correct, in that they represent a very accurate measure of the true structural response. In this case, we can further assume that  $\Omega_E = \Omega_T \equiv \Omega$ .

The problem to be addressed now is how to best combine the available analytical model of the stiffness  $K_A$  with all available experimental data to obtain an updated stiffness  $K$  that is in some sense closer to the true  $K_T$ . Since  $\Omega_E$  has been assumed to be very accurate and  $M_A$  is the reference basis, the central issue is therefore how to obtain the best approximation to the true mode shape and stiffness. In practice, the solution of two multivariable constrained optimization problems is required, as follows.

### 2.2. Orthogonalization

The measured mode shape  $\Phi_E$  does not, in general, satisfy the theoretical requirement of orthogonality. However, it can be normalized and orthogonalized to satisfy this condition in some optimal way, which ensures that the corrected modes are closest to the measured ones in the weighted Euclidean sense. The exact task at hand is: given an  $n \times m$  measured mode shape matrix  $\Phi_E$  and a symmetric positive definite  $n \times n$  mass matrix  $M$ , find the  $n \times m$  matrix  $\Phi$  that minimizes the weighted Euclidean norm and simultaneously satisfies a weighted orthogonality condition. In symbolic form, we seek

$$\min \phi = \|N(\Phi - \Phi_E)\|, \quad \text{s.t. } \Phi^T M \Phi = I, \tag{5}$$

where the weighting matrix is most often (but not always, see [15]) taken to be  $N = M^{1/2}$ , and such that

$$\Phi_{Ei} = \tilde{\Phi}_{Ei}^T (\tilde{\Phi}_{Ei}^T M \tilde{\Phi}_{Ei}^T)^{-1/2}, \quad (6)$$

where  $\Phi_{Ei}$  is the  $i$ th column of the normalized mode shape matrix and  $\tilde{\Phi}_{Ei}$  is the  $i$ th column of the original measured mode shape matrix. Note also that  $\Phi_{Ei}$  represents the mode shape corresponding to the  $i$ th resonant frequency.

As previously shown [12], the required orthogonalization can be achieved using the Lagrange multiplier technique to obtain

$$\Phi = \Phi_E (\Phi_E^T M \Phi_E)^{-1/2}, \quad (7)$$

where the mode shape  $\Phi$  satisfies the weighted orthogonality condition established by Eq. (5) and is closest to the normalized measured mode shape  $\Phi_E$ .

### 2.3. Updated stiffness

The stiffness matrix for a real structure is symmetric and positive definite, which implies  $K \equiv LL^T$ . The updated stiffness can be obtained by minimizing its weighted distance from the analytical stiffness  $K_A$ , while satisfying the constraints imposed by the equation of motion. In symbolic form, we seek

$$\min d = \|W^{-1/2}(LL^T - K_A)W^{1/2}\|, \quad \text{s.t. } LL^T\{\Phi\} = \Omega^2[M]\{\Phi\}, \quad (8)$$

where  $W$  is a symmetric but otherwise arbitrary weighting matrix. For example, it could be the identity matrix, the analytical stiffness matrix, or the mass matrix. For the special case  $W = M$ , it has been shown that the expression for the updated stiffness matrix is [15]

$$K = K_A - K_A \Phi \Phi^T M - M \Phi \Phi^T K_A + M \Phi \Phi^T K_A \Phi \Phi^T M + M \Phi \Omega^2 \Phi^T M. \quad (9)$$

## 3. Application to wheat

### 3.1. Experiment

Spring wheat (*Triticum aestivum* L.) was grown in the greenhouse using standard horticultural techniques. All plants were grown in 4 L pots on the bench in a climate-controlled glasshouse at the USDA-ARS Research Center in Beltsville, MD. The germplasm for two nearly isogenic varieties was kindly donated by Dr. Ravi Singh at the CIMMYT (International Center for Maize and Wheat Improvement, in Mexico). The first variety was Kauz tall, which is typical of traditional tall wheats and is susceptible to wind-induced crop damage. The second variety was an elite cultivar called Kauz semidwarf, which can be considered typical of modern wheats and is resistant to wind-induced crop damage. In contrast to the tall variety, Kauz semidwarf has one allele (copy) of the Rht1 gene mutation. This gene is one of several similar genes almost universally present in commercially grown wheats due to its positive effects on wind tolerance and grain yield [16].

Selected stalks were tested in vivo at Zadok's Growth Stage 83–85 [22], i.e., at green maturity. The stem of potted plants was excited by the reciprocating pushrod of a shaker motor (Ling Dynamics V200) attached to the stem at a height corresponding to 20% of the total stem height. The horizontal displacement at this attachment point was varied sinusoidally within the range of  $\pm 0.5$  mm, and the driving frequency was varied systematically in order to identify resonant frequencies that locally maximized the lateral displacements of the vibrating stalk. The stalk motion was monitored using 60 Hz videophotography and dimensional analysis of the recorded motion was later performed using NIH Image analysis software. Standard techniques were used to determine the mass and geometry of the spike and of each of the hollow segments comprising the stem [2]. The apparatus used in this forced frequency response test is shown in Fig. 1.

The experimental approach allowed the first  $m$  ( $m \leq n$ ) resonant frequencies to be identified in the range of 0.5–30 Hz. The resulting set of resonant frequencies  $\omega_{Ei}$ , where  $i = 1$  to  $m$ , were assembled into a diagonal measured frequency matrix  $\Omega_E$  in accordance with Eq. (3). The measured horizontal displacements of up to 20 discernible features on the stem were fitted with a least-square polynomial [17]. The horizontal and angular displacements of each node on the stem (a node is the intersection of two adjacent segments) were then recovered from the fitting curves, and assembled into the  $n \times m$  measured mode shape matrix  $\Phi_E$ , in accordance with Eq. (4). Recall that  $n$  represented the dof of the system, and was equal to two times the number of internodes. As discussed earlier, the measured resonant frequencies were assumed to be very close to the true values. In contrast, the measured mode shape required normalization and orthogonalization as described earlier in Section 2.2.

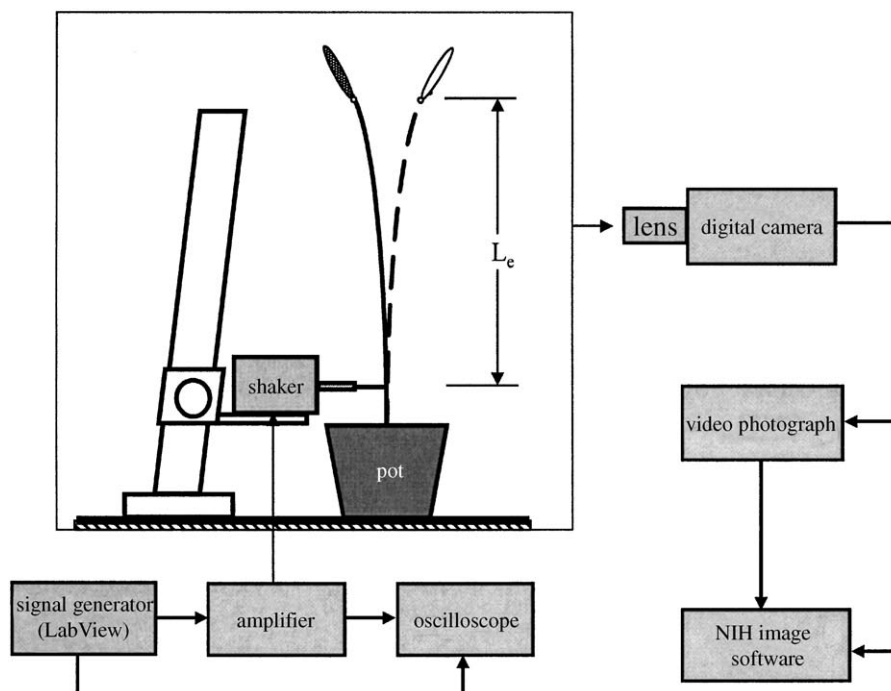


Fig. 1. Forced frequency response test apparatus.

### 3.2. Theoretical model

In the theoretical model, the stalk was idealized as a tube made up of several conjoined hollow cylinders (called internodes) of varying diameters and elastic moduli, which supported a heavy tip mass (called the spike). Referring to Fig. 2, the solid bulkheads that form the junctions between any two internodes are called nodes, and the structural configuration is similar to that of bamboo. Each internode is comprised of multiple layers of anisotropic

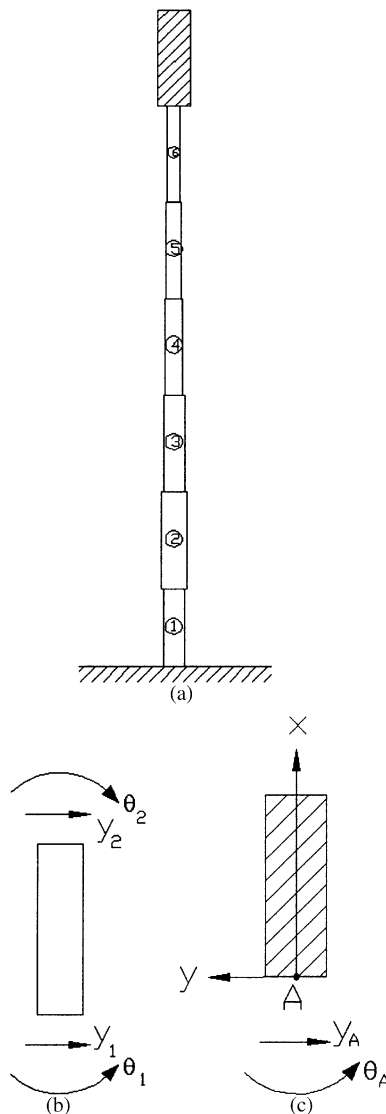


Fig. 2. Theoretical model of the heterogeneous structure of interest. A wheat stalk (a) consists of a hollow segmented stem comprised of 5 to 7 internodes, (b) supporting the grain-bearing spike. (c) Any given internode was assumed to have constant geometric and elastic material properties along its length.

water-saturated tissue. Even so, it is still reasonable to assume that its material behavior in flexure is elastic and can be characterized by an effective longitudinal modulus. This conception of a wheat stalk entails considerable simplification of the real structure, but captures some of its essential features. As a further approximation, each internode can be treated as a vertical beam element whose small deflection response is cubic. In effect, the total stem flexural behavior was therefore assumed to be piece-wise cubic in accordance with the finite element formulation summarized below. The bottom end of the stem was considered to be rigidly fixed in the ground. Due to the simple connectivity of this idealized model, each internode contributed two additional dof, that is, the horizontal and angular displacements of its upper end (Fig. 2(b)).

With these assumptions, the element mass and stiffness matrices obtained using the finite element method [18] are

$$m_e = \frac{\gamma_e l_e}{420} \begin{bmatrix} 156 & 22l_e & 54 & -13l_e \\ & 4l_e^2 & 13l_e & -3l_e^2 \\ \text{sym.} & & 156 & -22l_e \\ & & & 4l_e^2 \end{bmatrix} \tag{10}$$

and

$$k_e = \frac{E_e I_e}{l_e^3} \begin{bmatrix} 12 & 6l_e & -12 & 6l_e \\ & 4l_e^2 & -6l_e & 2l_e^2 \\ \text{sym.} & & 12 & -6l_e \\ & & & 4l_e^2 \end{bmatrix}, \tag{11}$$

respectively, where  $E_e$  is the longitudinal elastic modulus,  $I_e$  is the moment of inertia,  $l_e$  is the length, and  $\gamma_e$  is the weight per unit length of internode  $e$ , where  $e = 1$  to  $n_e$ . The maximum value of  $n_e$  varied between stalks in the range of 5–7. Here, the weight per unit length of each internode was calculated using its cylindrical geometry and an assumed specific weight of 0.9 (consistent with experimental observation).

Preliminary parameter study indicated that the model response was relatively insensitive to the precise value of the spike modulus. The spike was therefore considered to be a rigid cylinder rather than another flexible beam element. This simplification was advantageous because it avoided ill-conditioning of the total stiffness matrix [17]. The net contribution of the rigid spike to the total mass matrix was determined as follows. Referring to Fig. 2(c),  $y_A(t)$  and  $\theta_A(t)$  represent the time-varying linear and angular displacements of the lower end of the spike. When the maximum lateral stem deflections are small (as it was in the forced vibration test), the horizontal displacement on any vertical location  $x$  on the spike can be approximated as  $y_s = y_A + x\theta_A$ . And, if  $\gamma_s$  is the effective weight per unit length of an idealized cylindrical spike of length  $l_s$ , the kinetic energy of the oscillating spike is

$$T_s = \frac{\gamma_s}{2} \int_0^{l_s} (\dot{y}_A + x\dot{\theta}_A)^2 dx = \frac{\gamma_s}{2} (\dot{y}_A^2 l_s + l_s^2 \dot{y}_A \dot{\theta}_A + \frac{1}{3} l_s^3 \dot{\theta}_A^2). \tag{12}$$

The partial derivatives

$$\frac{d}{dt} \frac{\partial T_s}{\partial \dot{y}_A} = \gamma_s l_s \dot{y}_A + \frac{1}{2} \gamma_s l_s^2 \dot{\theta}_A \tag{13}$$

and

$$\frac{d}{dt} \frac{\partial T_s}{\partial \dot{\theta}_A} = \frac{1}{2} \gamma_s l_s^2 \dot{y}_A + \frac{1}{3} \gamma_s l_s^3 \dot{\theta}_A \tag{14}$$

were thus obtained, indicating that the spike mass matrix should be

$$m_s = \gamma_s \begin{bmatrix} 0 & 0 & 0 & 0 \\ 0 & 0 & 0 & 0 \\ 0 & 0 & l_s & \frac{1}{2} l_s^2 \\ 0 & 0 & \frac{1}{2} l_s^2 & \frac{1}{3} l_s^3 \end{bmatrix}, \tag{15}$$

where the effective spike length  $l_s$  and spike weight per unit length  $\gamma_s$  were again determined via simple experiments.

The total mass matrix  $[M_A]$  of dimension  $2n_e \times 2n_e$  was found by appropriate assembly of the individual internodal mass matrices (given by Eq. (10)) plus the spike mass matrix (given by Eq. (15)). Similarly, the total stiffness matrix  $[K_A]$  of dimension  $2n_e \times 2n_e$  was found by appropriate assembly of the individual internodal stiffness matrices (given by Eq. (11)).

Strictly speaking, the vibrating stalk could be treated as a very lightly damped forced system. However, its flexural response above the point of excitation was nearly identical to that of an equivalent undamped free system with the same stiffness and mass. Hence, the homogenous form of Eq. (2) was posed as a set of  $i$  eigenvalue problems

$$[K_A]\{\Phi_{Ai}\} - \omega_{Ai}^2 [M_A]\{\Phi_{Ai}\} = 0, \tag{16}$$

where the eigenvector  $\Phi_{Ai}$  is the analytical mode shape matrix and the associated eigenvalue  $\omega_{Ai}$  is the resonant frequency for the  $i$ th mode.

In this application, the individual entries in the banded analytical stiffness matrix could be defined symbolically using recursive formulae involving the material and geometric properties of each internode [2]. However, Eq. (16) could not be solved directly until some estimate of the unknown moduli of ultimate interest had been obtained. In practice, the stem moduli were initially assumed to vary linearly with height in order to obtain a first approximation of  $K_A$  that minimized the difference between the first two measured frequencies and the corresponding eigenvalues (but did not use any information about the measured mode shapes). Once this first estimate of  $K_A$  became available, a trial updated stiffness  $K$  could be found using Eq. (9). Then,  $K$  was iteratively refined using successive approximations of  $K_A$  based on progressively improved estimates of  $E_e$ , which were recovered from the diagonal entries of the previous  $K$ .



#### 4. Results

A systematic procedure based on the above theory was used to infer the longitudinal moduli of about 20 stalks representing both varieties. For clarity of presentation, selected results for only those stalks with exactly six internodes are presented below.

Fig. 3 shows the inferred moduli for each of five Kauz semidwarf stalks versus height. Each value is shown at the height corresponding to the geometric center of that internode. Since the theoretical model had assumed the moduli to be a constant within a given internode, these results are indicative of a step-wise variation with height. These in vivo material property data were derived from the true (updated) structural stiffness obtained using the reference basis method. Note that the fitting curves connecting each data do not have any direct physical interpretation. Similarly, Fig. 4 shows the inferred moduli for each of three Kauz tall stalks. Again, the value for each internode is shown at the height of its geometric center and the interpolated curves do not have any physical meaning. These material property data were also obtained by analysis of experimental frequency data using the reference basis model updating method.

To facilitate comparison of two varieties of differing height, Fig. 5 shows the average moduli of the same sample of eight stalks according to internode number. The moduli of both varieties were largest in the basal (lower) internode 1. However, the differences between the two varieties ( $\sim 6.3$  GPa for Kauz tall versus  $\sim 5.8$  GPa for Kauz semidwarf) were not statistically significant. Moving up through the middle internodes, the average moduli are steadily lower, and the differences between the two varieties reached significance at the 95% confidence level. The apical (or uppermost) internode 6 was comprised of the most flexible tissue and the differences in moduli between varieties ( $\sim 4.3$  GPa for Kauz tall versus  $\sim 2.9$  GPa for Kauz semidwarf) approached significance at the 99% confidence level. These results were selected from a larger sample that also included stalks with either five or seven internodes.

The elastic moduli inferred for these varieties of wheat were well within the range that has been defined by previous studies of non-woody plant tissues. Moreover, the nonlinear decrease in stem

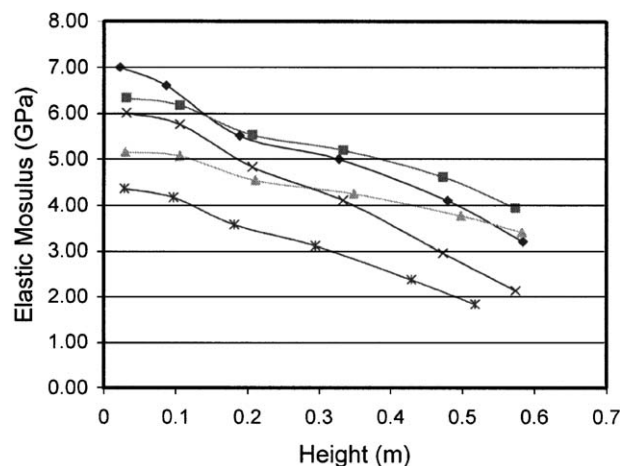


Fig. 3. Semidwarf wheat stem tissue moduli as a function of height. The inferred longitudinal moduli for each of six internodes are shown at the height corresponding to its geometric center, for each of five Kauz semidwarf stalks.

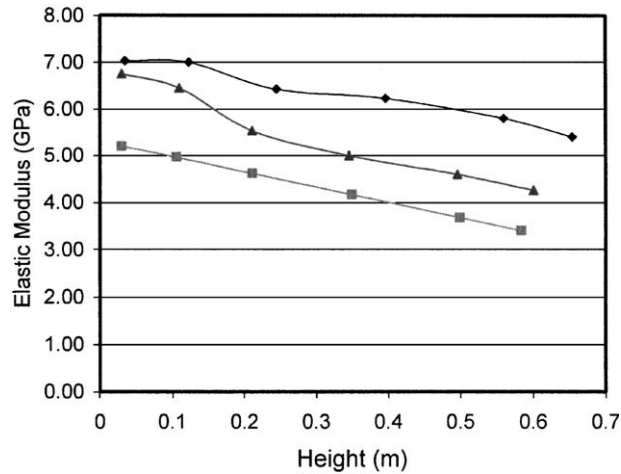


Fig. 4. Tall wheat stem tissue moduli as a function of height. The inferred longitudinal moduli for each of the six internodes versus height, for each of three Kauz tall stalks. The genetic background of this variety is identical to that of Kauz semidwarf except that it lacks the *Rht1* gene mutation.

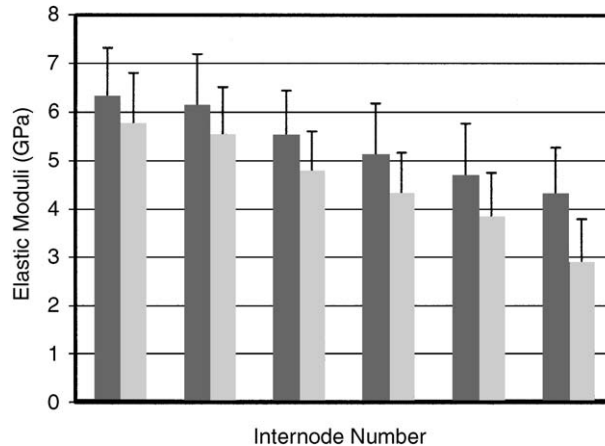


Fig. 5. Longitudinal elastic modulus versus internode number, for two contrasting varieties of wheat. The average (plus standard deviation) moduli of each internode are shown for Kauz tall (dark shading) and Kauz semidwarf (light shading). The differences between varieties are more significant in the apical or upper internodes.

tissue moduli with height was consistent with experimental results obtained by Zebrowski using ultrasonic wave speed measurements [5]. While the qualitative patterns established by that earlier study lend credence to the new results, this is the first study to provide a quantitative map of the in vivo height-wise variations in wheat stem tissue moduli. For this reason, the crucial step of model validation must rely on indirect supporting evidence, as discussed below.

## 5. Discussion

The results indicated that the internodal tissue closest to the ground exhibited an effective longitudinal modulus approaching the value reported for wood (e.g., 11 GPa for Douglas fir [19]). This is plausible since the basal stem of wheat is partially lignified and experiences the highest levels of wind-induced bending stress. In contrast, the tissue of both varieties, especially Kauz semidwarf, was considerably more flexible in the upper stem. Again, this was consistent with expectation, and reflects the optimization trade-off between stem rigidity versus aeroelasticity. As discussed elsewhere, the latter is thought to enhance the wind tolerance of many elite semidwarf varieties in comparison to traditional tall varieties [20].

Eq. (9) does not require any particular number of frequencies or mode shapes to obtain estimates of  $E_e$ . One might expect that increasingly accurate estimates of the moduli would be obtained as additional high-frequency information was included in the model updating process. In fact, the improvement was very minor and was similar to the resolution of the frequency response data (i.e.,  $\sim 1\%$ ) in this study. In fact, a trial stiffness matrix could be formulated using only the first two resonant frequencies, and the updating process could then be performed using only the first resonant frequency and mode shape. In practice, it was determined that estimates of  $E_e$  obtained on this basis were very similar to those that were obtained when all of the available frequency response information (i.e., up to 4 frequencies and modes less than 30 Hz) was included in the process. To illustrate this point, Fig. 6 shows the percentage change in the average internodal moduli of Kauz semidwarf, when the updating process was based on the first two modes rather than the fundamental mode only. These results showed that the values of the predicted moduli were hardly affected by the inclusion of higher frequency data, which implied that the updated model changed very little, consistent with the findings of an earlier report [21].

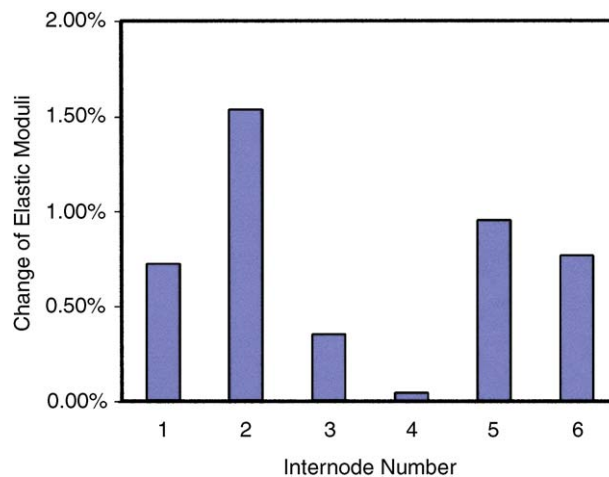


Fig. 6. Change in predicted moduli as number of mode shapes used for model updating increases. The figure shows the change in the predicted modulus of each internode as the number of mode shapes used for model updating was increased from one to two. In this and other applications in which the fundamental mode shape can be determined with accuracy, higher order mode shape data may have very little effect on the outcome of the updating process.

The reference basis method made it possible to obtain a reasonably accurate estimate of spatially varying material properties based entirely on the first few modes of vibration. In essence, this was possible because the fundamental and second mode shapes were known with relatively high level of accuracy. It is likely that this useful observation can be generalized to many engineering applications. It implies that the relatively easy measurements of large-amplitude, low-frequency mode shapes can capture enough information to permit accurate spatial mapping of material property data. In many cases, this may obviate the need to perform the more difficult measurements of smaller amplitude, higher frequency response. Alternately, when such information is also available, as it was in the present application, it can provide a redundant check on the validity of the updated model.

As might be expected, the updated resonant frequencies obtained using two mode shapes were not exactly the same as the measured frequencies. Interestingly, this need not be understood to imply that the moduli determined from the updated model were less than accurate. Referring to Table 1, observe that the true fundamental frequency was slightly higher than the measured value.

Table 1  
True versus measured resonant frequencies in first three flexural modes

Predicted frequency (Hz)	Measured frequency (Hz)
1.09	1.02
7.86	7.90
21.20	20.50

The measured frequencies were found by video dimensional analysis and the true (i.e., updated) resonant frequencies were found by reference basis model updating.

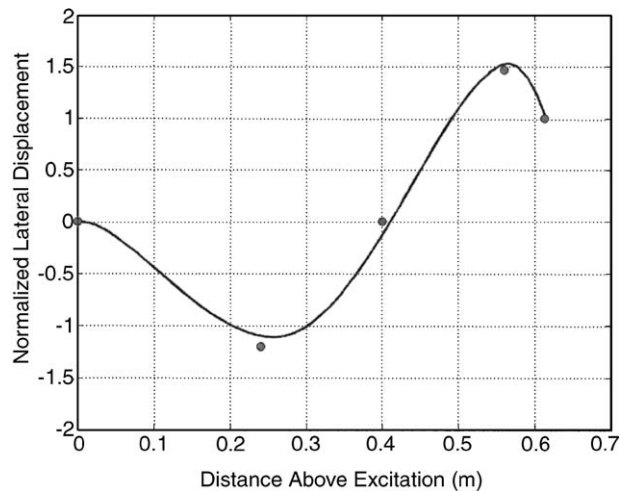


Fig. 7. Third mode shape of updated model compared with experimental data. The continuous curve is the third mode shape of the updated model based on the first two resonant frequencies and modeshapes. The dots are the actual displacements of selected locations on the vibrating stem at resonance. Remarkably, the updating process improves the accuracy with which the material property data of ultimate interest can then be determined.

This was almost certainly due to the imprecise theoretical approximation of the lower boundary condition as rigidly fixed. In fact, the degree of fixation provided by the alligator clamp attaching the reciprocating pushrod to the basal stem was unknown. Similarly, the true second resonant frequency was slightly lower than the measured value. Again, this was almost certainly due to the imprecise theoretical assumption of spike rigidity. To further illustrate this point, Fig. 7 compares the updated and measured third mode shapes. The overall match is reasonably compelling, but the updated shape is that of a stem that is slightly less compliant at its lower end, and slightly more compliant at its upper end, in comparison to observation. The qualitative differences in measured versus predicted mode shape were sufficiently large that the updated stem moduli were substantially different from those obtained using the original theoretical model. Remarkably, the nature of the shift in system response that occurs during the updating process is such that the updated behavior is more similar to the experimental response that would occur if the theoretical model were correct, than the actual structural response! Thus, as demonstrated in this unusual application of frequency response analysis, the reference basis model updating process can improve the accuracy with which the intrinsic material properties of vibrating structure can be determined.

## References

- [1] P.W. Heisey, P. Aquino, V. Hernandez, E. Rice, *CIMMYT 1995/96 World Wheat Facts and Trends, Chapter Part 2: The current World Wheat Situation*, Mexico, D.F. CIMMYT, 1996.
- [2] T. Farquhar, J. Zhou, H. Meyer, Rht1 dwarfing gene selectively decreases the material stiffness of wheat, *Journal of Biomechanics*, In press, 2004.
- [3] M. Neenan, J.L. Spencer-Smith, An analysis of the problem of lodging with particular reference to wheat and barley, *Journal of Agricultural Science* 85 (3) (1975) 495–507.
- [4] G. Skubisz, Zeszyty problemowe postepow nauk rolniczych, Chapter: The determination of the Young's Modulus of a stalk of winter wheat on the basis of field and laboratory measurements, *International Conference on Physical Properties of Plant Materials and Their Influence on Technological Processes*, 1978.
- [5] J. Zebrowski, Complementary patterns of stiffness in stem and leaf sheaths of triticale, *Planta* 187 (1992) 301–305.
- [6] M.J. Crook, A.R. Ennos, Mechanical differences between free standing and supported wheat plants, *triticum aestivum l. Annals of Botany* 77 (1996) 197–202.
- [7] M.J. Crook, A.R. Ennos, The effect of nitrogen and growth regulators on stem and root characteristics associated with lodging in two cultivars of winter wheat, *Journal of Experimental Botany* 46 (289) (1995) 931–938.
- [8] H.-Ch. Spatz, T. Speck, Local buckling and other modes of failure in hollow plant stems, *Biomimetics* 2 (1994) 149–173.
- [9] J. Zebrowski, The use of free vibration to measure peduncle stiffness in triticale, *Journal of Experimental Botany* 42 (1991) 1207–1212.
- [10] J. Zebrowski, Dynamic behavior of inflorescence-bearing triticale and triticum stems, *Planta* 207 (1999) 410–417.
- [11] J.E. Mottershead, M.L. Friswell, Model updating in structural dynamics: a survey, *Journal of Sound and Vibration* 167 (1993) 347–375.
- [12] M. Baruch, Optimization procedure to correct stiffness and flexibility matrices using vibration tests, *AIAA Journal* 16 (1978) 1208–1210.
- [13] M. Baruch, Y. Bar Itzhack, Optimal weighted orthogonalization of measured modes, *AIAA Journal* 16 (1978) 346–351.
- [14] A. Berman, E.J. Nagy, Improvement of a large analytical model using test data, *AIAA Journal* 21 (1983) 1168–1173.
- [15] R. Kenigsbuch, Y. Halevi, Modal updating in structural dynamics: a generalized reference basis approach, *Mechanical System and Signal Processing* 12 (1998) 75–90.

- [16] H.M. Phillips, Dynamic structural behavior of wheat as a function of Rht dwarfing gene dose, Master Thesis: University of Maryland, Baltimore County, 2001.
- [17] J. Zhou, Constrained optimization of the dynamic structural performance of *Triticum aestivum* L. (wheat), Ph.D. dissertation, University of Maryland, Baltimore County, 2003.
- [18] M.L. James, *Vibration of Mechanical and Structural Systems*, second ed., Harper Collins, New York, 1994.
- [19] J.E. Shigley, C.R. Mischke, *Mechanical Engineering Design*, sixth ed., McGraw-Hill, New York, 2001.
- [20] T. Farquhar, H. Meyer, J. van Beem, Effect of aeroelasticity on the aerodynamics of wheat, *Materials Science & J Engineering C: Biomimetic Materials, Sensors and Systems* 7 (2000) 111–117.
- [21] A. Berman, Inherently incomplete finite element model and its effects on model updating, *AIAA Journal* 38 (2000) 2142–2146.
- [22] J.C. Zadoks, T.T. Chang, C.F. Konzak, A decimal code for the growth stages of cereals, *Weed Research* 14 (1974) 415–421.